INSTITUTE OF PHYSICS PUBLISHING PLASMA PHYSICS AND CONTROLLED FUSION

Plasma Phys. Control. Fusion **46** (2004) 869–876 PII: S0741-3335(04)69853-8

Marginal stability diagrams for infinite-n ballooning modes in quasi-symmetric stellarators

S R Hudson[1], **C C Hegna**[2], **R Torasso**[3] **and A Ware**[4]

[1] Princeton Plasma Physics Laboratory, PO Box 451, Princeton, NJ 08543, USA
[2] Department of Physics, University of Wisconsin-Madison, Madison, WI 53706, USA
[3] Courant Institute of Mathematical Sciences, New York University, NY 10012, USA
[4] Department of Physics and Astronomy, The University of Montana, MT 59812, USA

Received 3 October 2003
Published 5 April 2004
Online at stacks.iop.org/PPCF/46/869
DOI: 10.1088/0741-3335/46/5/009

Abstract

By varying the pressure-gradient and average shear at a selected surface in a given arbitrary stellarator equilibrium and by inducing a coordinate variation such that the perturbed state remains in equilibrium, a family of magnetohydrodynamic equilibria local to the surface is constructed. The equilibria are parameterized by the pressure-gradient and averaged magnetic shear. The geometry of the surface is not changed. The perturbed equilibria are analysed for infinite-n ballooning stability and marginal stability diagrams are constructed that are analogous to the (s, α) diagrams constructed for axisymmetric configurations.

The method describes how pressure and rotational-transform gradients influence the local shear, which in turn influences the ballooning stability. Stability diagrams for the quasi-axially symmetric NCSX, a quasi-poloidally symmetric configuration and the quasi-helically symmetric HSX are compared. Regions of second-stability are observed in both NCSX and the quasi-poloidal configuration, whereas no second-stable region is observed for the quasi-helically symmetric device.

To explain the different regions of stability, the curvature and local shear of the quasi-poloidal configuration are analysed. The results are seemingly consistent with the following simple explanation: ballooning instability results when the local shear is small in regions of bad curvature with sufficient pressure-gradient. Examples will be given that show that the structure and stability of the ballooning mode is determined by the structure of the potential function arising in the Schrödinger form of the ballooning equation.

1. Introduction

By employing the standard WKB-like formulation, the leading order stability of high-k ideal modes in stellarator plasmas is governed by an ordinary differential equation, the ballooning

 © 2004 IOP Publishing Ltd Printed in the UK

equation [1]. The ballooning equation shows that it is the interaction of pressure-gradients, curvatures and the local shear that determines ballooning stability.

The local pressure-gradient at a given surface affects directly the ballooning stability. A cursory investigation of ballooning stability suggests that, as the magnitude of pressure-gradient is increased, ballooning modes can only be destabilized. This however is not the case. The local shear also influences ballooning stability, and the local shear is related to the pressure-gradient through the Pfirsch–Schlüter currents. As the pressure-gradient is increased at a given surface with fixed geometry, the local shear must change to preserve the magnetohydrodynamic (MHD) equilibrium condition. Depending on the geometry of the surface, it may be the case that the local shear will be altered in such a manner as to stabilize infinite-n ballooning modes. This effect has been studied in axisymmetric equilibria [2] and is called 'second-stability'.

In addition to this effect, as the ratio of averaged plasma energy to averaged magnetic energy, β, is increased, the global equilibrium properties will be modified. For example, as β is increased, geometrical deformations associated with the Shafranov shift will alter the curvature. This in turn will alter the ballooning stability properties. However, as the following results will verify, this is a smaller effect than the impact on ballooning stability associated with the variations in the local shear.

The primary interest of this paper is to examine the phenomena of second-stability in stellarator geometry. Hegna and Nakajima [3] extended the method of profile variations introduced by Greene and Chance [2] to stellarator geometry. This method allows the pressure-gradient and average magnetic shear to change at a given surface but keeps the surface geometry unchanged. The MHD equilibrium condition is used to determine the self-consistent change in the local shear. This technique allows the variations in ballooning stability caused by variations in the local shear to be distinguished from the variations in ballooning stability caused by the geometrical change associated with increasing β.

It will be shown that the method of profile variations and the marginal stability diagrams thus constructed give an accurate indication of the stability limits for a variety of stellarator configurations.

2. Profile variations

This section will outline the method of profile variations in stellarator geometry. For full details the reader is referred to Hegna and Nakajima [3]. Further discussion and details of the numerical implementation are given by Hudson and Hegna [4]. The magnetic field is given in Boozer coordinates [5]:

$$\boldsymbol{B} = \nabla\psi \times \nabla\theta + \iota(\psi)\nabla\zeta \times \nabla\psi = h(\psi,\theta,\zeta)\boldsymbol{\nabla}\psi + I(\psi)\boldsymbol{\nabla}\theta + G(\psi)\boldsymbol{\nabla}\zeta. \tag{1}$$

For the contravariant and covariant forms to be equivalent, there are several metric identities that must be satisfied. One such identity is obtained by taking the dot product of the two forms for $\boldsymbol{B}$: the coordinate Jacobian must satisfy $\sqrt{g} = (G + \iota I)/B^2$. Such metric identities and the equilibrium condition $\nabla p = \boldsymbol{J} \times \boldsymbol{B}$ are used to derive consistency relations among varied quantities.

Given such a representation for the field, it is then the coordinate transformation $\boldsymbol{x}(\psi,\theta,\zeta)$ itself that determines the MHD equilibrium. The method of profile variations will impose a variation in the pressure and rotational-transform profiles and calculate the coordinate response required to preserve the MHD equilibrium condition.

The pressure and rotational-transform profiles are described in the vicinity of a selected magnetic surface ψ_b by the expansion

$$p(\psi) = p^{(0)}(\psi) + \mu p^{(1)}(y) + \cdots, \qquad \iota(\psi) = \iota^{(0)}(\psi) + \mu\iota^{(1)}(y) + \cdots, \tag{2}$$

where $p^{(0)}$ and $\iota^{(0)}$ are the pressure and rotational-transform profiles of the undisturbed equilibrium, $p^{(1)}$ and $\iota^{(1)}$ are the perturbation profiles and $\mu \ll 1$ is a small expansion parameter. The auxiliary variable $y = (\psi - \psi_b)/\mu$ is used to ensure that the variations in the gradients of the pressure and rotational-transform are of lower order than the variations in the pressure and rotational-transform. The gradients of the pressure and rotational-transform take the form

$$p'(\psi) = p^{(0)\prime}(\psi) + p^{(1)\prime}(y) + \cdots, \qquad \iota'(\psi) = \iota^{(0)\prime}(\psi) + \iota^{(1)\prime}(y) + \cdots. \tag{3}$$

The coordinate transformation is perturbed similarly:

$$\boldsymbol{x}(\psi, \theta, \zeta) = \boldsymbol{x}^{(0)}(\psi, \theta, \zeta) + \mu \boldsymbol{x}^{(1)}(y, \theta, \zeta) + \cdots. \tag{4}$$

The perturbed basis vectors are

$$\boldsymbol{e}_\psi = \boldsymbol{e}_\psi^{(0)} + \partial_y \boldsymbol{x}^{(1)} + \cdots, \qquad \boldsymbol{e}_\theta = \boldsymbol{e}_\theta^{(0)} + \mu \partial_\theta \boldsymbol{x}^{(1)} + \cdots, \qquad \boldsymbol{e}_\zeta = \boldsymbol{e}_\zeta^{(0)} + \mu \partial_\zeta \boldsymbol{x}^{(1)} + \cdots. \tag{5}$$

For consistency, both G and I are perturbed in a manner similar to that of p and ι, but h requires order unity variations. The lowest order quantity in the coordinate variation is $\partial_y \boldsymbol{x}^{(1)}$. This quantity can be expanded in the following basis set,

$$\frac{\partial \boldsymbol{x}^{(1)}}{\partial y} = C\boldsymbol{B} + D\frac{\boldsymbol{B} \times \boldsymbol{\nabla}\psi}{B^2} + M\frac{\boldsymbol{\nabla}\psi}{g^{\psi\psi}}, \tag{6}$$

where C, D and M are to be determined. An expression for C is obtained from the momentum balance equation. By requiring that the magnetic field strength be undisturbed to lowest order gives the condition $M = 0$. An equation for the term D can be obtained and solved numerically for a given equilibrium from the lowest order perturbed momentum balance equation and Ampere's Law,

$$\begin{aligned}\partial_\eta D = {} & \iota^{(1)\prime}\frac{1}{\oint 1/g^{\psi\psi}}\left(\frac{1}{g^{\psi\psi}} - \oint \frac{1}{g^{\psi\psi}}\right) - p^{(1)\prime}\frac{V'(G + \iota I)}{\oint 1/g^{\psi\psi}} \\ & \times \left(\frac{\lambda}{g^{\psi\psi}}\oint \frac{1}{g^{\psi\psi}} - \frac{1}{g^{\psi\psi}}\oint \frac{\lambda}{g^{\psi\psi}}\right),\end{aligned} \tag{7}$$

where $\partial_\eta = \partial_\zeta + \iota\partial_\theta$, λ is related to the Pfirsch–Schlüter currents and $4\pi^2 \oint q \equiv \oint\oint q \, \mathrm{d}\theta \, \mathrm{d}\zeta$ is the flux surface average. The function D depends on the original equilibrium; more precisely, the terms multiplying $\iota^{(1)\prime}$ and $p^{(1)\prime}$ depend only the selected surface of the original equilibrium. Once these terms have been computed, a simple task given the Fourier representation of the equilibrium, no further equilibrium calculations are required.

As far as the infinite-n ballooning equation is concerned, the only quantity that is affected by the profile variations, in addition to p' and ι', is the local shear, $s \equiv (\boldsymbol{b} \times \boldsymbol{n}) \cdot \nabla \times (\boldsymbol{b} \times \boldsymbol{n})$, where $\boldsymbol{b}$ and $\boldsymbol{n}$ are, respectively, the unit vectors along the magnetic field and normal to the magnetic surface. We can separate the contributions to s into a flux surface averaged quantity, the global shear, ι', and the variation of the local shear, $\tilde{s}$. The quantity D describes the variation in local shear due to changes in the two profile quantities. The perturbed part of the local shear takes the simple form

$$\frac{G\partial_y \boldsymbol{x}^{(1)} \cdot \boldsymbol{e}_\theta - I\partial_y \boldsymbol{x}^{(1)} \cdot \boldsymbol{e}_\zeta}{\sqrt{g}g^{\psi\psi}} = D. \tag{8}$$

The term D thus represents how the profile variations affect the local shear. This coordinate variation function, described by D, is a crucial point of the second-stability properties of the stellarator. The increased pressure-gradient, in addition to increasing the de-stabilizing interaction with the unfavourable curvature, alters the local shear, which is the dominant stabilizing mechanism.

The ballooning mode equation in the perturbed equilibrium is written by transforming the angle variables $\alpha = \theta - \iota\zeta$, $\eta = \zeta$ so that α labels the field line, η labels position along the field line and the $\boldsymbol{B}\cdot\nabla$ operator becomes $\boldsymbol{B}\cdot\nabla = \sqrt{g}^{-1}\partial_\eta$. The ballooning equation is given in a form that highlights the role of the (integrated) local shear,

$$\frac{\partial}{\partial\eta}\Lambda\frac{\partial}{\partial\eta}\xi + 2(p^{(0)\prime} + p^{(1)\prime})\sqrt{g}(G + \iota I)(\kappa_n + \kappa_g L)\xi = \gamma(\psi, \alpha, \eta_k)\Lambda\xi, \tag{9}$$

where $\Lambda = (B^2/g^{\psi\psi} + g^{\psi\psi}L^2)$, L is the integrated local shear $L = \int_{\eta_k}^{\eta} \mathrm{d}\eta' s(\eta')$, η_k is the ballooning angle and $\gamma = -\omega^2$ is the ballooning eigenvalue, where ω is the growth rate of the instability, which in general depends on the surface, field line and ballooning angle, η_k. This is an ordinary differential equation with boundary condition $\xi(\pm\infty) = 0$. For numerical work, the boundary condition is that $\xi(\eta_k \pm \eta_\infty) = 0$, where η_∞ is chosen sufficiently large to contain the mode.

The ballooning equation may be written in Schrödinger form, $[\mathrm{d}^2/\mathrm{d}\vartheta^2 + E - V]\Lambda^{1/2}\xi = 0$, where the 'potential', $V(\vartheta)$, depends on the coefficients of the ballooning equation [6]

$$V = \frac{\mathcal{K}}{\Lambda} - \frac{1}{4\Lambda^2}\left(\frac{\mathrm{d}\Lambda}{\mathrm{d}\vartheta}\right)^2 + \frac{1}{2\Lambda}\frac{\mathrm{d}^2\Lambda}{\mathrm{d}\vartheta^2}, \tag{10}$$

where $\mathcal{K} = 2p'\sqrt{g}(G + \iota I)(\kappa_n + \kappa_g L)$ is the de-stabilizing term. The structure of the Schrödinger potential determines the structure of the eigenfunction. Intuition obtained from the quantum theory suggests that if the potential has high barriers then the mode will more likely be localized.

The profile variations describe the separate effects that the variation in p' and ι' have on the local shear and thus on ballooning stability. Taking p' and ι' as independent variables, a two-dimensional family of equilibrium surfaces may be constructed from a single numerically computed (VMEC) equilibrium. The ballooning stability may be determined for each of the perturbed equilibria and marginal stability curves constructed. Note that if the analysis of the perturbed equilibrium is local to the original surface, ψ_b, as infinite-n ballooning analysis indeed is, then the equations describing how the variations affect the local shear are exact. Variations of any magnitude are allowed, and the stability properties of the perturbed equilibria are characteristic of the geometry of the original surface.

3. Stability diagrams, local shear and curvature

In figure 1 are shown the stability diagrams for the NCSX [7] configuration *li*383, the quasi-poloidal configuration *m*3*b*15 [8] and the HSX standard configuration [9] *hsxstd*. This selection reflects the current US interest in quasi-symmetric devices. From this figure it is clear that the second-stability properties of stellarators can vary considerably.

As predicted by Hegna and Hudson [10], the quasi-helically symmetric configuration *hsxstd* does not display a second-stable region. The quasi-axisymmetric configuration *li*383 does display a second-stable region, but it is quite weak in the sense that very high $\beta \approx 16\%$ is required to access this region. The quasi-poloidal symmetric configuration *m*3*b*15 shows a strong second-stable region, as observed by Ware *et al* [8].

For all the configurations, as β is increased, there is some change in the stability diagrams. This assumedly is the result of geometric distortions of the surfaces. Nonetheless, it has been confirmed that the stability diagrams give a good quantitative prediction of the marginal β limit, and the qualitative agreement is very good.

To analyse the physical cause of ballooning instability and the mechanism leading to second-stability, the *m*3*b*15 and *hsxstd* configurations are examined. First, numerical evidence supporting the claim that ballooning instability results when regions of small shear coincide

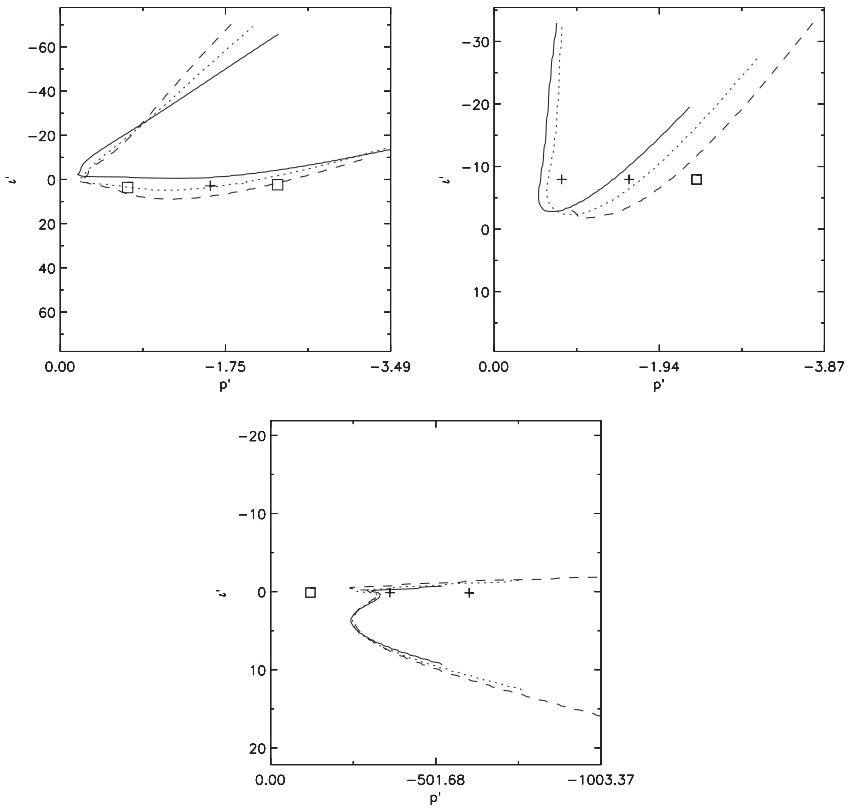

Figure 1. Marginal stability diagrams for (top left) *li*383 VMEC surface $s = 0.6$—$\beta = 4.2\%$ (——), $\beta = 9.5\%$ (· · · · · ·) and $\beta = 14.0\%$ (- - - -); (top right) *m*3*b*15 VMEC surface $s = 0.3$—$\beta = 1.2\%$ (——), $\beta = 2.4\%$ (· · · · · ·) and $\beta = 3.7\%$ (- - - -); (bottom) *hsxstd* VMEC surface $s = 0.6$—$\beta = 0.7\%$ (——), $\beta = 2.2\%$ (· · · · · ·) and $\beta = 3.6\%$ (- - - -). Each stability diagram is centred on the original surface, the location of which is shown with '+' if the surface is unstable and '□' if that surface is stable.

with regions of bad curvature is presented. Variations in the pressure-gradient at the $s = 0.3$ VMEC surface of the *m*3*b*15 equilibrium at $\beta = 2.4\%$ have been imposed. The pressure-gradient variations are chosen to place the resulting equilibria in the first stable region, the unstable region and the second-stable region, and this provides a clear illustration of the effect of the variations in the local shear. Examination of the ballooning equation suggests that the de-stabilizing influences on ballooning modes is the product of the pressure-gradient with the normal and geodesic curvature, and the stabilizing influence arises from large shear. In figure 2 is shown the normal curvature, scaled by the pressure gradient $|p'|\kappa_n$; the geodesic curvature, scaled by the pressure gradient, $|p'|\kappa_g$; the local shear, s, and the ballooning eigenvalue, γ, for the first-stable, unstable and second-stable equilibria.

Within the context of the method of profile variations, the curvature does not change, but as the magnitude of the pressure-gradient increases, regions of bad curvature (indicated in red) will result in a greater de-stabilizing effect. The local shear does change as a result of the profile variations. In figure 2, regions of small local shear (indicated in red) represent regions where the stabilizing force is weak. Both the curvature components and the local shear are functions of position (θ, ζ). Finally in figure 2, the ballooning eigenvalue is shown, where red

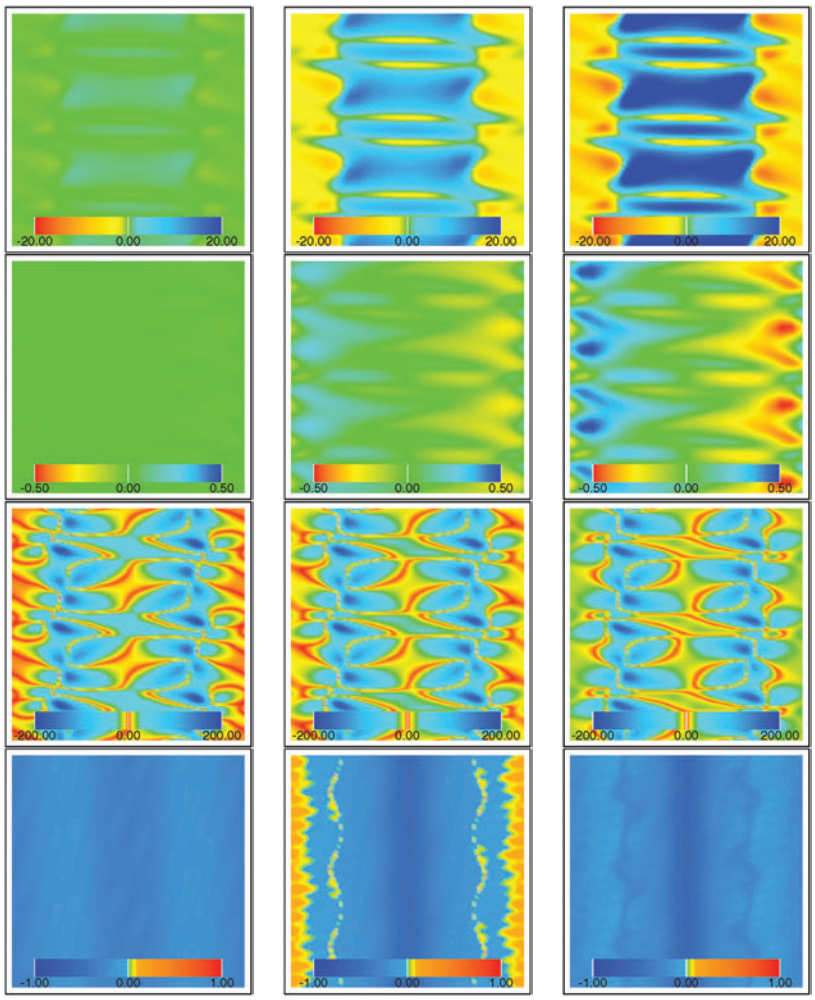

Figure 2. Mechanism of ballooning instability for the $m3b15$ $\beta = 2.4\%$ configuration on VMEC surface $s = 0.3$. From top to bottom: $|p'|\kappa_n$; $|p'|\kappa_g$; local shear s; and ballooning eigenvalue γ. From left to right: the first-stable region $(\iota^{(1)\prime}, p^{(1)\prime}) = (0.0, 1.502)$; the unstable region $(\iota^{(1)\prime}, p^{(1)\prime}) = (0.0, 0.404)$; and the second-stable region $(\iota^{(1)\prime}, p^{(1)\prime}) = (0.0, -0.694)$. The poloidal angle is horizontal, and the toroidal angle is vertical.

(This figure is in colour only in the electronic version)

indicates instability and blue represents stability. To express the ballooning eigenvalue as a function of position on the surface, the field line label, α, and the ballooning eigenvalue, η_k, have been chosen to match (θ, ζ). Figure 2 shows that ballooning instability results, in this case, when small local shear coincides with an unfavourable normal combined with large pressure-gradients. The mechanism for second-stability is that the pressure-induced parallel currents alter the local shear, which in turn alters the correlation between regions of small local shear and unfavourable curvature. In the second-stable case, even though the pressure-gradient has increased, the contour of zero local shear has shifted towards a less de-stabilizing region on the flux surface and the stabilizing effect of shear has strengthened in the poor curvature region: this is the mechanism of second-stability.

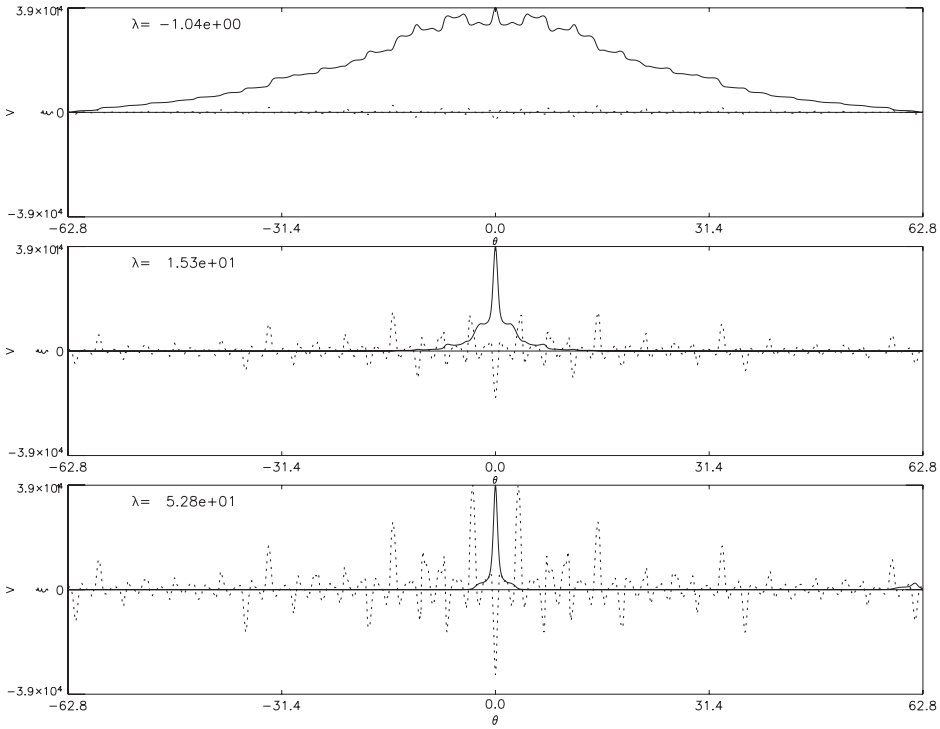

Figure 3. Schrödinger potential (- - - -) and eigenfunction (——) for *hsxstd* $\beta = 2.2\%$ on VMEC surface $s = 0.6$ configuration for $(\iota^{(1)\prime}, p^{(1)\prime}) = (0.0, 300.0)$ (top), $(0.0, 0.0)$ (middle) and $(0.0, -300.0)$ (bottom).

To illustrate both the relationship between the Schrödinger potential and ballooning stability and to compare the *m*3*b*15 case, which has a strong second-stable region, with the *hsxstd* case, which does not possess a second-stable region, the Schrödinger potential for various cases are shown in figures 3 and 4. There is a clear connection between the structure of the potential and the structure of the ballooning eigenfunction. The peaks in the potential cause the eigenfunction to localize and thus become unstable.

For the *hsxstd* case, as the pressure-gradient is increased, the peaks in the potential increase seemingly without limit. Consequently, as the pressure-gradient is increased, the tendency of the eigenfunctions to localize becomes greater and there is no second-stable region. For the *m*3*b*15 case, the selected variations in the pressure-gradient place the equilibria in the first-stable, unstable and second-stable regions. The peaks in the potential function do not increase. In fact, as the pressure-gradient is increased, the peaks in the potential diminish and allow the eigenfunction to broaden and stabilize. We expect that an analysis of the potential function arising in the Schrödinger form of the ballooning equation may provide an insightful method for understanding ballooning instability.

4. Conclusion

The method of profile variations is a efficient means of determining the stability of a family of equilibria nearby a numerically computed equilibrium. It provides a good qualitative understanding and prediction of the stability properties that are characteristic of the geometry

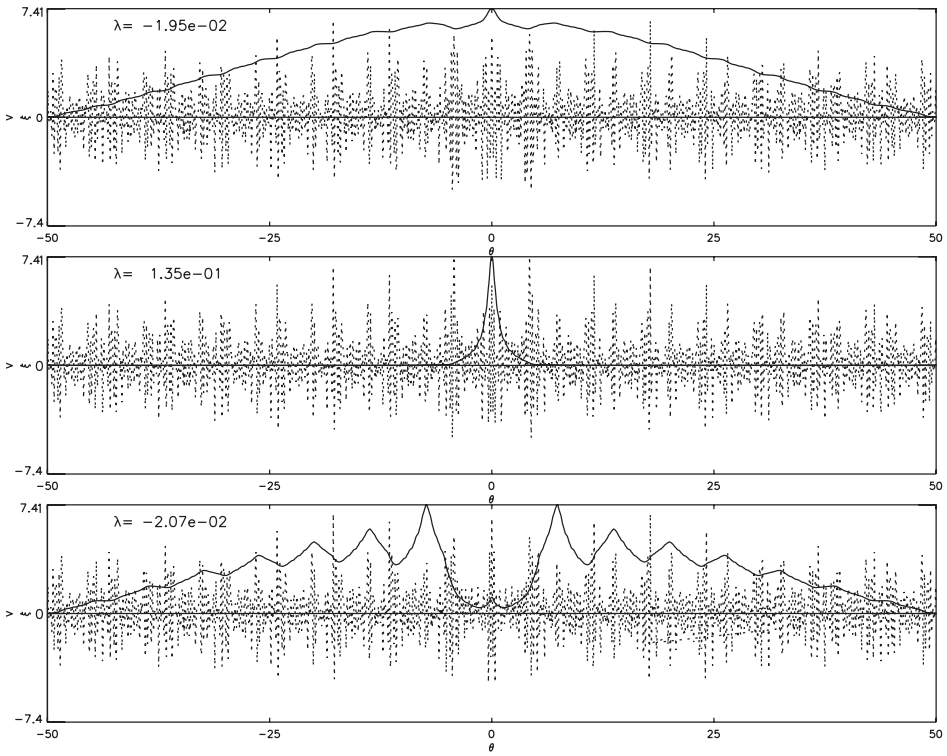

Figure 4. Schrödinger potential (- - - -) and eigenfunction (——) for $m3b15$ $\beta = 2.4\%$ on VMEC surface $s = 0.3$ configuration for $(\iota^{(1)\prime}, p^{(1)\prime}) = (0.0, 1.502)$ (top), $(0.0, 0.404)$ (middle) and $(0.0, -0.694)$ (bottom).

of the equilibrium. The observations are consistent with the suggestion that ballooning modes will localize in regions of small local shear and bad curvature. Variations in the pressure-gradient will alter the local shear and thus change where the local shear is small. In some cases, this can lead to stabilization of ballooning modes as pressure is increased.

Acknowledgment

This work supported in part by US DOE contract AC02-76CH0-3073.

References

[1] Dewar R L and Glasser A H 1983 *Phys. Fluids* **26** 3038
[2] Greene J M and Chance M S 1981 *Nucl. Fusion* **21** 453
[3] Hegna C C and Nakajima N 1998 *Phys. Plasmas* **5** 1336
[4] Hudson S R and Hegna C C 2003 *Phys. Plasmas* **10** 4716
[5] Boozer A H 1982 *Phys. Fluids* **25** 520
[6] Cuthbert P and Dewar R L 2000 *Phys. Plasmas* **7** 2302
[7] Zarnstorff M C *et al* 2001 *Plasma Phys. Control. Fusion* **43** A237
[8] Ware A S *et al* 2002 *Phys. Rev. Lett.* **89** 125003-1
[9] Talmadge J N and Cooper W A 1996 *Phys. Plasmas* **3** 3713
[10] Hegna C C and Hudson S R 2002 *Phys. Plasmas* **9** 2014